Taylor & Francis
Taylor & Francis Group

Journal of Adhesion Science and Technology

ISSN: 0169-4243 (Print) 1568-5616 (Online) Journal homepage: http://www.tandfonline.com/loi/tast20

Chitosan Schiff base as eco-friendly inhibitor for mild steel corrosion in 1 M HCl

R. Menaka & S. Subhashini

To cite this article: R. Menaka & S. Subhashini (2016): Chitosan Schiff base as eco-friendly inhibitor for mild steel corrosion in 1 M HCl, Journal of Adhesion Science and Technology, DOI: 10.1080/01694243.2016.1156382

To link to this article: http://dx.doi.org/10.1080/01694243.2016.1156382

Published online: 21 Mar 2016.

JOURNAL OF ADHESION SCIENCE AND TECHNOLOGY, 2016
http://dx.doi.org/10.1080/01694243.2016.1156382

Taylor & Francis
Taylor & Francis Group

Chitosan Schiff base as eco-friendly inhibitor for mild steel corrosion in 1 M HCl

R. Menaka and S. Subhashini

Department of Chemistry, Avinashilingam Institute for Home Science and Higher Education for Women, Coimbatore, India

ABSTRACT

In the present study, natural biopolymer chitosan was modified into its Schiff base derivative with salicylaldehyde by condensation method. The prepared chitosan salicylaldehyde Schiff base was characterized using ultraviolet spectroscopy, fourier transform infrared spectroscopy, scanning electron microscope and elemental analysis. Thermal analysis was also carried out to determine the thermal stability of the derivative. To explore the corrosion inhibition performance of the chitosan Schiff base, weight loss, and electrochemical techniques were conducted. The inhibitor reduces the metallic corrosion by adsorbing on to the metal surface. The adsorption of chitosan Schiff base on mild steel surface in 1 M HCl follows Temkin isotherm model. Thermodynamic parameters of adsorption and corrosion process were calculated, which revealed the chemical nature of adsorption. SEM and energy dispersive X-ray spectroscopic analysis confirmed the formation of protective chitosan derivative layer on the mild steel surface.

ARTICLE HISTORY
Received 4 December 2015
Revised 9 February 2016
Accepted 10 February 2016

KEYWORDS
Chitosan; Schiff base; corrosion; Temkin; chemisorption; SEM analysis

1. Introduction

Mild steel (MS) is a major component in many of the industrial equipment due to its mechanical properties and economical significance. But it gets corroded when exposed to aggressive environment like acid during industrial processes. The corrosion products are removed by pickling with acids above room temperature. Hydrochloric acid is commonly used pickling acid in industries up to 60 °C. To reduce the metal attack during this process, corrosion inhibitors are widely used. Due to high toxicity and environmental regulation restrictions, the researchers are diverted to focus on developing environmentally safe and biodegradable corrosion inhibitors. Various researchers had reported that the natural products, amino acids, natural polymers, medicinal drugs, etc. exhibit efficient inhibition towards corrosion process.[1–6] Natural polymers are considered to be the most promising corrosion inhibitors because of the nontoxicity, biodegradability, easy availability, and cost-effectiveness. In recent years, a number of naturally occurring polymers such as pectin, starch, guar gum, and gum Arabic. have been investigated

CONTACT S. Subhashini subhashini_chem@avinuty.ac.in

as corrosion inhibitors in different corrosive environments.[7–12] Umoren and Eduok have reviewed the metal protection applications of carbohydrate polymers and their derivatives.[13]

Recently, chitosan a second abundant natural resource have received a considerable attention due to its good environmental profile. It is *N*-deacetylated product of chitin, an attractive material with biocompatibility and biodegradability having wide range of applications in medicine, wastewater treatment, environmental protection, textiles, cosmetics, and many other industrial sectors. Chitosan is rich in hydroxyl groups and amino groups which can act as a good inhibitor and few literatures have reported about its corrosion inhibition.[14–16] Both reactive amino and hydroxyl group present in the chitosan offers better corrosion inhibition through ionic interactions with metal surface. Some authors have also been discussed about the inhibition performance of chitosan derivatives in acid media.[17,18] The two reactive groups of the chitosan can be chemically modified into its derivative under mild reaction conditions. One among the modification is the formation of Schiff base by the reactions of free amino group of chitosan with an active carbonyl groups of aldehydes. Chemical modification of chitosan has resulted into much improvement in their corrosion inhibition efficiency. The effect of chitosan–crotonaldehyde Schiff base in 3% NaCl solution was studied for metal alloy and its behavior was reported by Mohammed and Fekry[19].

The present work aims on the modification of chitosan into a Schiff base and its application as corrosion inhibitor for MS in 1 M HCl. To study the metal corrosion behavior in acid solution, conventional weight loss technique at 303–343 K and at different immersion time were carried out along with electrochemical techniques. The surface morphology of MS was analyzed for the corrosion inhibition of chitosan Schiff base for MS in acid medium.

2. Experimental

2.1. Materials

Chitosan (75% deacetylated, Himedia), salicylaldehyde (Avra), acetone (99%) (Avra), hydrochloric acid, and ethanol.

2.2. Synthesis of chitosan Schiff bases

About 1 g of chitosan was dissolved in 100 ml of 1% acetic acid; and 1 ml of salicylaldehyde in 10 ml of ethanol was added in drops to the chitosan solution with constant stirring at room temperature. The stirring was continued for 7 h. The resultant yellow solution was kept overnight. The product was precipitated using acetone and washed several times to remove unreacted aldehydes.

2.3. Characterization of chitosan Schiff bases

Chitosan and modified chitosan were analyzed using Fourier transform infrared spectroscopy (FTIR) (Schimadzu IR affinity 1). Thermal behavior of chitosan and its Schiff base was studied using thermogravimetric analyzer (EXSTAR SII TG/DTA 6300). The elemental composition was calculated using Elemental vario EL III. Ultraviolet (UV) spectra were recorded using UV spectrophotometer 2202 (systronics). The surface morphology was analyzed by scanning electron microscopy (JEOL JSM-6490LA).

2.4. Material preparation for corrosion study

Corrosion studies (weight loss) were conducted with commercially available MS strips of dimension 5 cm × 1 cm × 2 mm and electrochemical studies with of 1 cm^2 coupons of the composition of C-0.106%, Mn-0.196%, P-0.027%, Cr-0.022%, S-0.016%, Ni-0.012%, Si-0.006%, Mo-0.003%, and remainder Fe. The MS specimens were mechanically polished, their surface was abraded with fine grade emery paper, degreasing in acetone and stored in desiccator at room temperature before conducting experiments.

2.5. Weight loss experiments

Weight loss experiments were carried out following standard ASTM G31procedure.[20] Weighed MS specimens were immersed in the absence and presence of different concentrations of inhibitor in 100 ml of 1 M HCl solution at different immersion periods (1–24 h) and at various temperatures (303–343 K). MS specimens were removed, cleaned, dried, and weighed. From the weight loss values obtained the corrosion rate and inhibition efficiency were calculated using the following equations,

$$CR(mpy) = \frac{3.45 \times 10^6 \times W}{ADt}$$

$$IE(\%) = \frac{Wo - W}{Wo} \times 100$$

where Wo and W are the weight loss (g) of the coupon in the absence and presence of inhibitor, A is the area of the coupon in cm^2, D is the density of the material in g/cm^3, and t is the time of exposure in hours.

2.6. Electrochemical studies

Electrochemical measurements were performed in a conventional three electrode glass cell using Potentiostat/galvanostat (Solartron 1280B) supported with corrware and Zplot softwares. A MS specimen with exposed area of 1 cm^2 as working electrode, saturated calomel electrode, and platinum electrode was used as reference and counter electrode, respectively. Prior to the experiments, the working electrode was polished with different grades of emery paper, rinsed with distilled water and then inserted to the glass cell. The working electrode was allowed to immerse in the electrolyte solutions for about 15 min to attain the steady state potential. Potentiodynamic polarization curves were obtained from anodic potential of −0.1 V to cathodic potential of −1 V vs. open circuit potential at a sweep rate of 2 mV/s. Electrochemical impedance spectroscopy (EIS) measurements were carried out at a frequency range of 20 kHz to 0.1 Hz by applying AC amplitude of 10 mV. The results were collected using Z plot software and interpreted with Z view software.

2.7. Surface analysis using scanning electron microscope (SEM)

Surface morphology of mildsteel specimens immersed in absence (1 M HCl) and presence of inhibitor (1500 ppm) were examined by SEM JEOL JSM-6490LA.

3. Results and discussion

3.1. Characterization of chitosan Schiff bases

FTIR spectrum of chitosan salicylaldehyde Schiff base (CHSA) was shown in the Figure1. The strong absorption band at 1631.83 cm^{-1} is attributed to C=N vibrations characteristic of imines [21,22] formed due to the condensation reaction between the amino group of chitosan and carbonyl group of salicylaldehyde. The absorption peaks at 1112.96 and 1067.64 cm^{-1} correspond to the polysaccharide moiety.[21,23,24] The peak at 1579.75 cm^{-1} corresponds to the N–H bending in secondary amides.[25] This absorption is also attributed to the C = C stretching in the aromatic ring of the aldehyde.[22–24]The peaks at 1494.88 and 1456.30 cm^{-1} are assigned to the characteristic absorbance of phenyl ring.[21]

The elemental compositions of the chitosan and the chitosan Schiff base are presented in the Table 1. The increase in carbon, hydrogen content of the Schiff base derivative suggest the condensation of salicylaldehyde on the chitosan chain. The increase in the C/N ratio also confirms the substitution.

Thermogravimetric analysis of the CHSA was conducted to measure their weight loss at different temperatures in the heating range of 40–550 °C at a heating rate of 10 °C per minute. Thermograph of chitosan and Schiff base polymer show two degradation stages

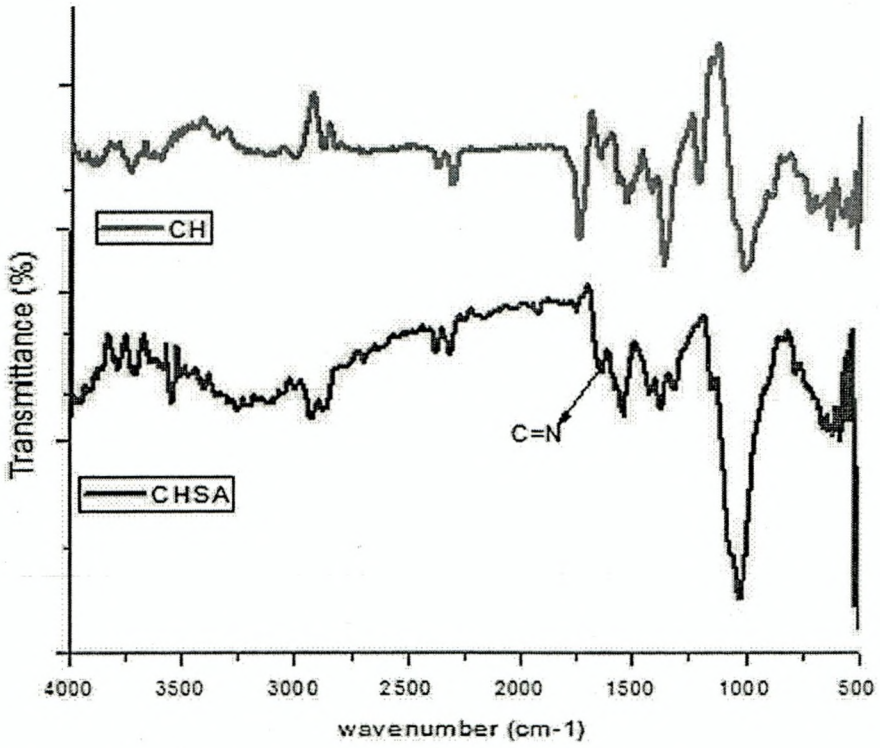

Figure 1. FTIR spectra of Chitosan and Chitosan salicylaldehyde Schiff base.

Table 1. Elemental analysis of chitosan and the chitosan Schiff base.

Sample	C	H	N	C/N
CH	39.71	7.48	7.16	5.55
CHSA	52.02	8.25	6.04	8.62

which is shown in Figure 2. The first decomposition step is due to loss of water molecule. The second decomposition step occurs in the range of 230–350 °C is due to degradation of polymers. The thermal degradation step of Schiff base indicates that Schiff base polymer is less stable than the chitosan. The instability of the Schiff base polymer than chitosan is attributed to the formation of imines (–N=CH–) groups in the polymer matrix.

The UV visible spectrum of chitosan Schiff base is shown in Figure 3. Chitosan Schiff base polymer in aqueous solution exhibits broad peak at the region 215–350 nm due to the presence of π bond(–N=CH–). This characteristic region is absent in chitosan which confirms the formation of imine group in the polymer chain.

The SEM micrographs of chitosan and its Schiff base are shown in Figure 4(a and b), respectively. Chitosan had a non porous, flat, and smooth surface. Chitosan Schiff base showed a noticeable wrinkles and porous structure which reveals the formation of Schiff base on the chitosan matrix.

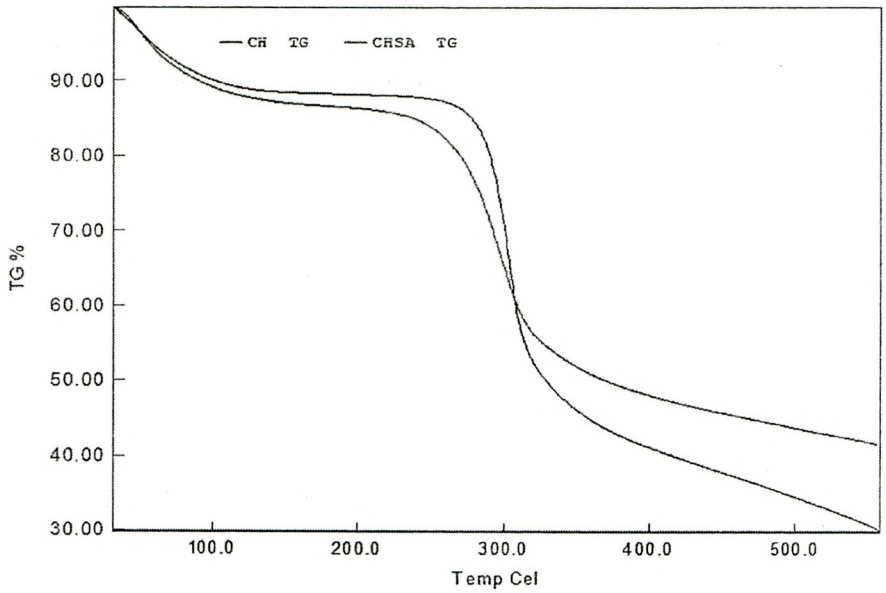

Figure 2. Thermographs of chitosan and chitosan Schiff base.

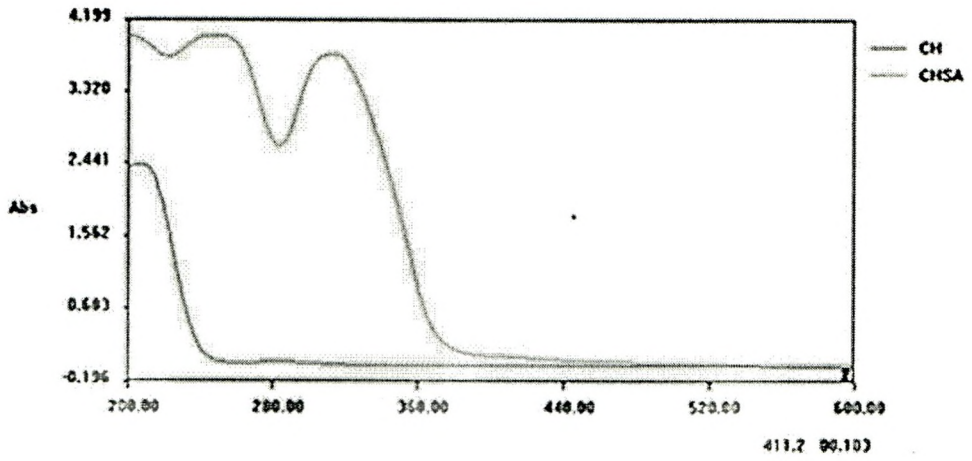

Figure 3. UV spectra of chitosan and chitosan Schiff base.

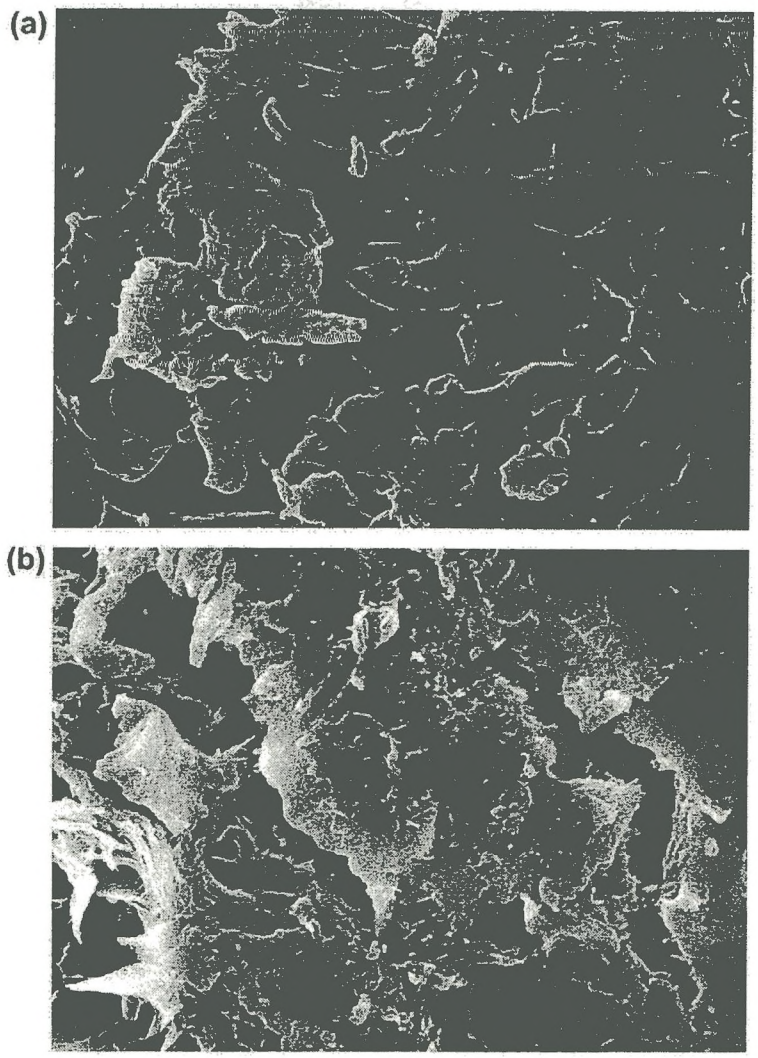

Figure 4. SEM images of (a) Chitosan (b) Chitosan salicylaldehyde schiff base.

3.2. EIS measurements

EIS technique, a non-destructive technique was employed to study the nature of the electrochemical processes that occurs at the metal/1 M HCl interface and also to understand the influence of chitosan Schiff base on metal dissolution process. Figure 5(a) shows the impedance spectra for MS in acid medium in presence and absence of different concentrations of chitosan Schiff base. Figure 5(b and c) represents the corresponding bode and phase angle plots of chitosan Schiff base, respectively. The Nyquist plots exhibit the single depressed capacitive loop over the frequency range studied and the diameter of the loop increased with increase in the concentration of inhibitor. This implies that the metal dissolution process is controlled by single transfer process that is unaffected by the addition of inhibitor molecules.[26,27] The increase in the diameter of the loop suggests that the MS corrosion is inhibited by forming a protective layer on the metal surface. The similar shape of Nyquist plot reveals that the corrosion mechanism is unaffected by the addition of chitosan Schiff base. The electrochemical impedance parameters such as solution resistance (*Rs*) and charge transfer resistance (*Rct*) were obtained by fitting the impedance spectra and tabulated in Table 2. The equivalent circuit shown in Figure 5(a) is used for fitting the impedance data.

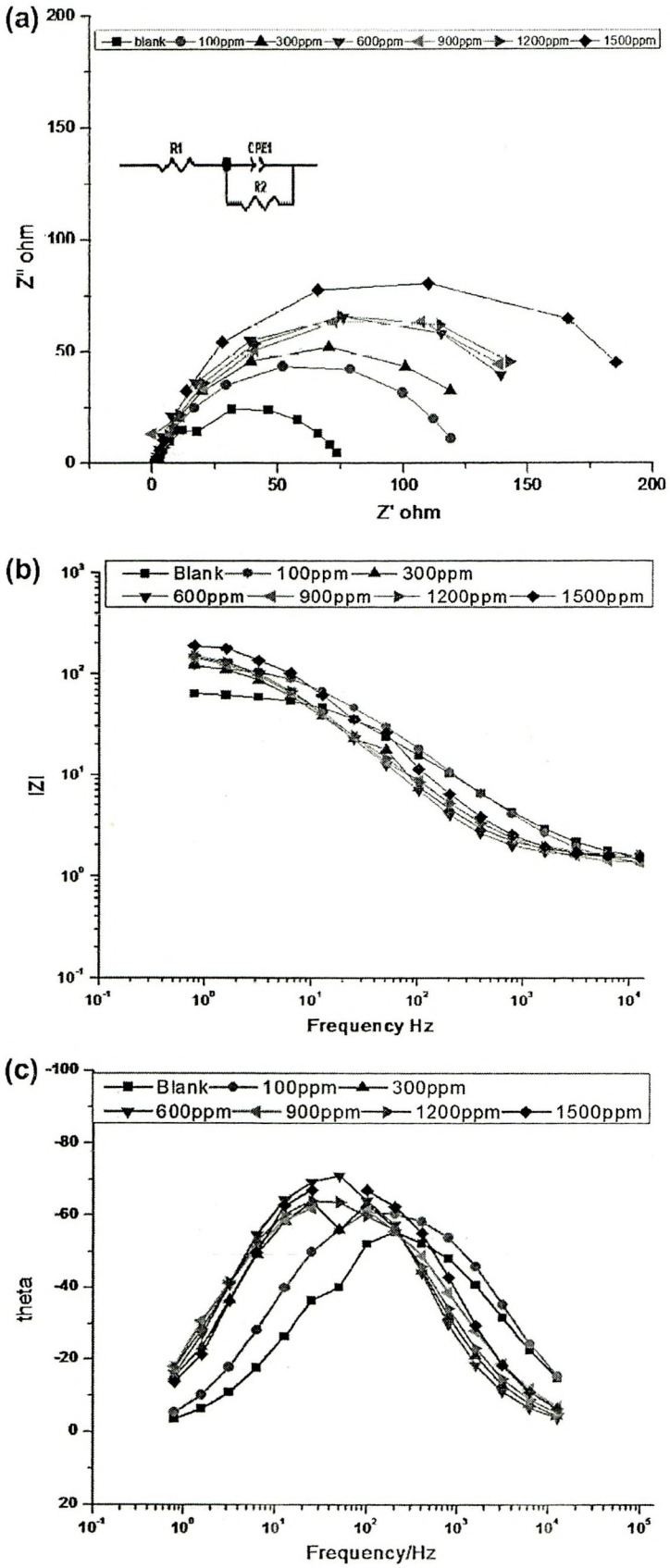

Figure 5. (a) Impedance curves (b) Bode plots (c) Phase angle plot of chitosan Schiff base.

Table 2. Impedance parameters for MS in 1 M HCl in presence and absence of chitosan Schiff base.

Concentration (ppm)	Rs (Ωcm^2)	*n*	Yo*10^{-6}	*Rct* (Ωcm^2)	Chi-Sqr	*IE*%
Blank	1.369	0.76427	416.60	63.44	0.0022891	
100	1.201	0.80096	307.90	122.7	0.00053398	48.30
300	1.538	0.84107	577.79	133.9	0.01333	52.62
600	1.547	0.89866	462.60	156.1	0.00051841	59.36
900	1.326	0.81926	628.35	169.9	0.02112	62.66
1200	1.588	0.83234	586.58	172	0.00040809	63.12
1500	1.33	0.84199	382.23	212	0.13967	70.08

The *IE* was determined from the *Rct* values by the following equation,

$$IE\% = \frac{Rct - Rct'}{Rct} \times 100$$

The *Rct* values for the inhibited system is higher when compared to the uninhibited which is due to the reduction in metal dissolution and the increased *Rct* values with an increase in concentration attributed to the higher surface coverage of the inhibitors on the MS surface. The obtained values of *n* are in the range of $0.5<n>1$, is an evidence for the surface roughness and inhomogeneity of the electrode surface.[28,29]

3.3. Polarization techniques

Figure 6(a) shows the OCP curve for MS in 1 M HCl. The attainment of steady state potential at short immersion period is due to the rapid dissolution of MS in acid medium. The potentiodynamic polarization curves for MS in 1 M HCl in presence and absence of different concentrations of chitosan Schiff base was shown in Figure 6(b). From the Figure 6(b), it can be seen that both the cathodic and anodic current densities decrease by the addition of chitosan Schiff base. This indicates the hindering attack of the chitosan Schiff base on the MS corrosion in 1 M HCl. Values of electrochemical parameter namely, corrosion current density (I_{corr}), corrosion potential (E_{corr}), anodic, and cathodic Tafel slopes and inhibition efficiency are listed in Table 3.

The polarization curves indicate that both the anodic metal dissolution and cathodic hydrogen evolution reactions are affected by the addition of chitosan Schiff base suggesting the mixed nature of the inhibition. Also, the parallel nature of the tafel lines suggests the activation-controlled hydrogen evolution reaction.[30] The displacement in the E_{corr} value is less than 85 mV is also an evidence for the chitosan Schiff base to function as mixed type inhibitor. I_{corr} values decreases with the increase in concentration which is due to the blocked fraction of MS surface by adsorption.[31,32] Thus, the polarization and impedance results are in good agreement.

3.4. Weight loss study – effect of immersion time

The performance of chitosan Schiff base was investigated with different immersion time (1–24 h) to monitor the metal dissolution process. The variation of *IE* with different immersion period for different concentration of chitosan Schiff base is shown in Figure 7(a). Inhibition efficiency increases as the immersion time increases attains a maximum *IE* of 91% at 24 h of immersion time. The inhibition effect is due to the formation of adsorption

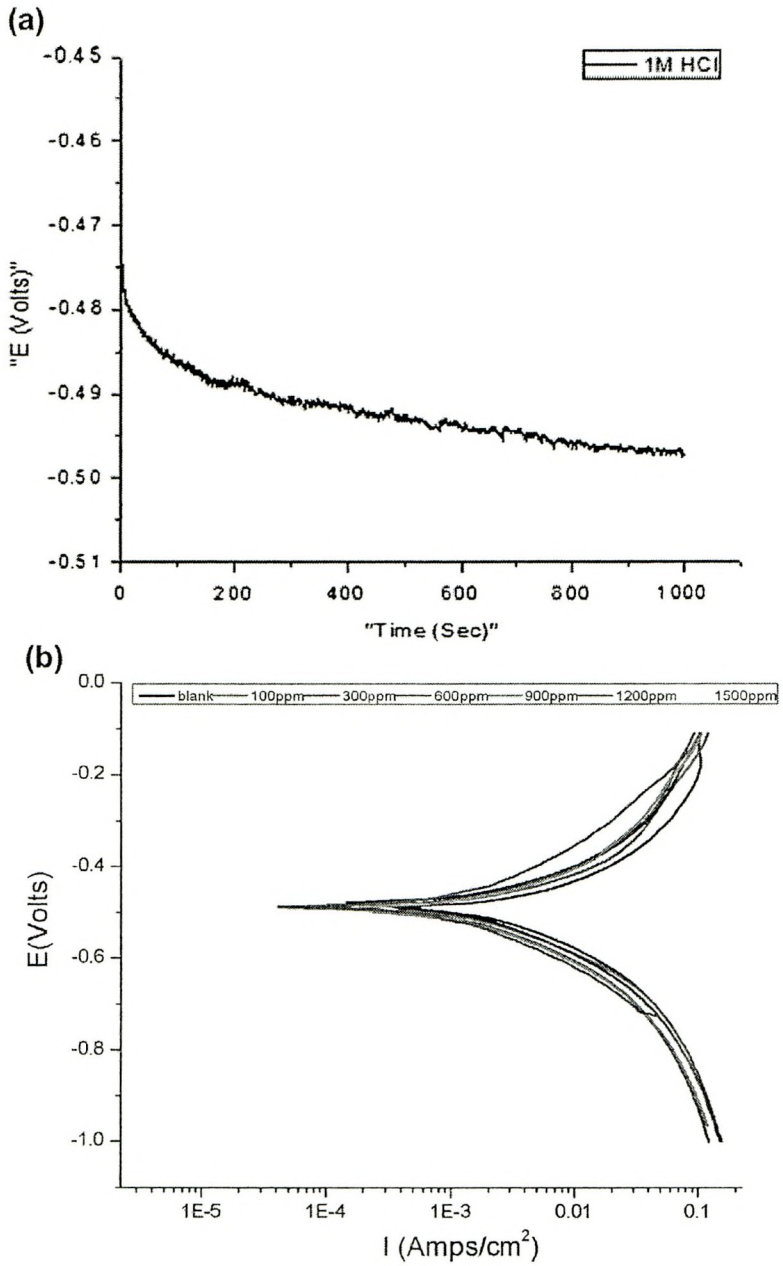

Figure 6. (a)Plot of OCP vs time for mild steel in 1M HCl, (b) Polarization curves for mild steel in 1M HCl in absence and presence of chitosan Schiff base.

Table 3. Polarization parameters for MS in 1 M HCl in presence and absence of chitosan Schiff base.

Concentration (ppm)	ba (mV/decade)	bc (mV/decade)	I_{corr} (mA/cm²)	*IE* I_{corr} (%)	Rp Ωcm²	*IE* Rp (%)	E_{corr} mV/SCE
Blank	163.92	132.2	4.1748		6.51		−495.45
100	150.84	109.89	2.3471	43.78	9.05	28.04	−485.93
300	123.39	102.66	1.3758	67.05	15.30	57.47	−487.21
600	131.21	100.84	1.2279	70.59	16.63	60.86	−486.67
900	129.67	101.63	1.0832	74.06	20.02	67.49	−485.31
1200	118.55	95.335	0.8485	79.68	19.70	66.96	−485.93
1500	101.78	88.835	0.3965	90.50	26.40	75.35	−485.42

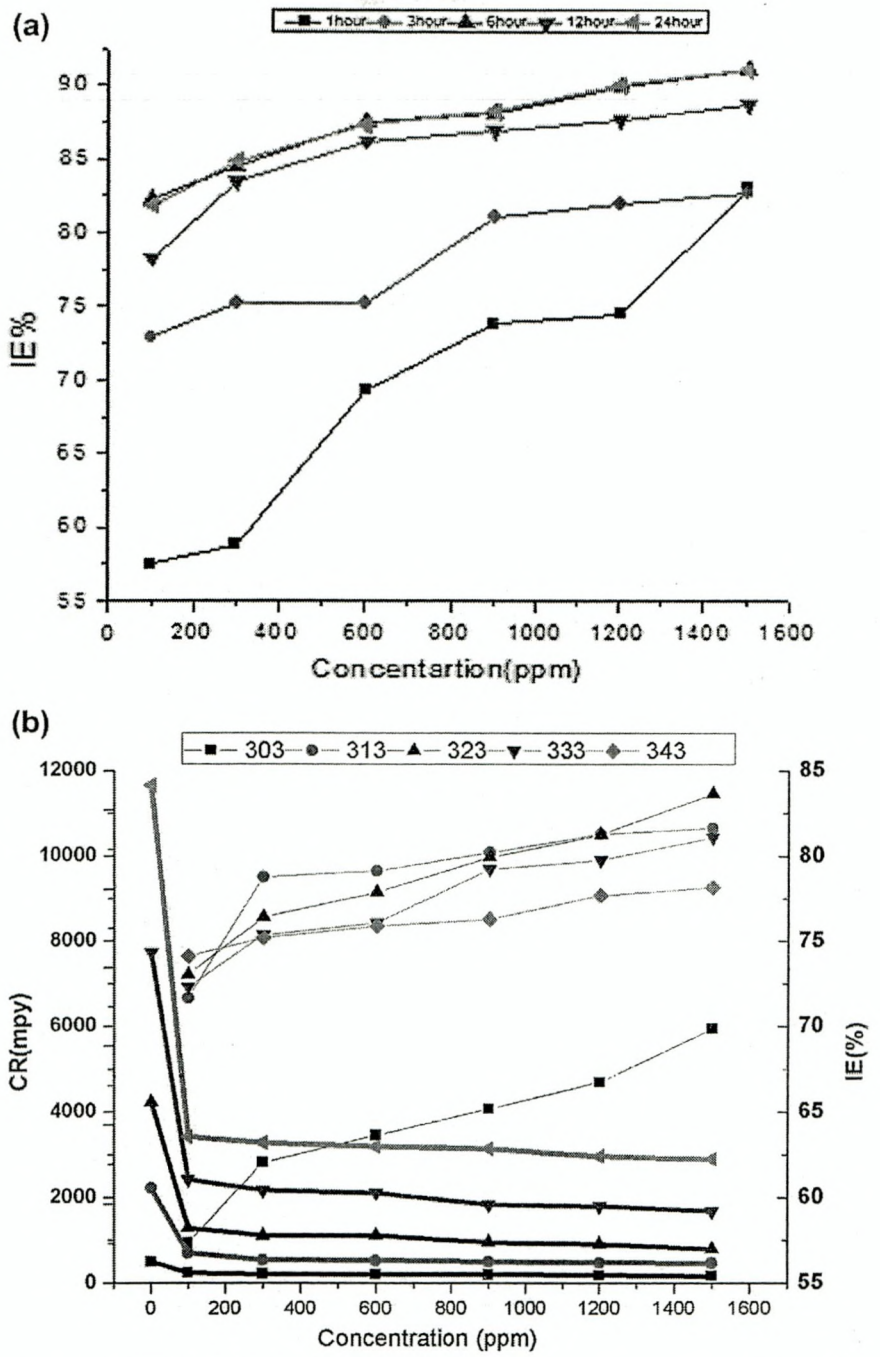

Figure 7. (a)Variation of inhibition efficiency for different concentration of inhibitor at different immersion periods, (b)Trend of corrosion rate and inhibition efficiency at temperatures 303-343K.

layer on the metal surface. The higher inhibition may be attributed to the film forming capability of the chitosan derivative and also its greater stability towards the acid attack.

3.4.1. Effect of temperature

Temperature plays an important role in corrosion monitoring technique since it helps to determine the nature of adsorption of inhibitor on the metal surface. Increase in inhibition efficiency on increasing the temperature is associated with chemisorption and the reverse is

associated with physisorption. The effect of temperature on the corrosion inhibition of MS in 1 M HCl was evaluated in presence of different concentration of CHSA by weight loss experiment. Figure 7(b) reveals the trend of corrosion rate and inhibition efficiency on the temperature domain studied. It can be seen that the *IE* increases with increase in inhibitor concentration at 303 K. This may be attributed to the fact that the formation of polymeric Schiff base layer at MS/ HCl solution interface.[33] Further inspection of the Figure 7(b) revealed that the corrosion rate increases with the increase in temperature in inhibited and uninhibited solutions. Also there was decrease in corrosion rate and increase in *IE* on the addition of different concentrations of chitosan Schiff base.

The *IE* was found to increase with the inhibitor concentration for all the studied temperature (313–343 K). From the Figure 7(b), it is clear that the *IE* increases with temperature up to 333 K and decrease at temperature 343 K. This fact may be explained by the structural orientation of the polymer as mentioned by Geethanjali.[29] The long chains of the polymer adsorb on to the metal surface at lower temperature and thereby reducing the corrosion rate. The increase in temperature from 313–333 K may break the adsorbed long chains of the polymer into smaller segments. At higher temperature (343 K), these smaller segments of the polymer desorbs from the metal surface, resulting in lesser *IE*. The decrease in the *IE* at higher temperature also confirms that the adsorption–desorption process is shifted towards desorption process at 343 K. This may be also due to the roughening of the metal surface thereby reducing the ability of the inhibitor to adsorb on the metal surface resulting in enhanced corrosion.[33] On the other hand, the increase in the *IE* with the increase in temperature could augment the chemical interaction between the inhibitor molecule and the metal surface leading to higher surface coverage.[34]

3.5. Thermodynamic activation parameters

Temperature influence on the corrosion rate can be evaluated through the activation parameters using Arrhenius equation:

$$log\ CR = -\frac{E_a}{2.303RT} + \log A$$

where *CR* is the corrosion rate, *A* is the Arrhenius constant, *R* is the molar gas constant, and *T* is the absolute temperature. Activation energy values (E_a) obtained from the slope of the linear plot of log *CR* against $1/T$ is given in Table 4. The calculated values of activation energy for the blank 1 M HCl found to be 62 kJ mol^{-1} which is in correlation with literature values 50–100 kJ mol^{-1}. The E_a value decreases in presence of inhibitor compared to blank. Decrease in the E_a can be attributed to an appreciable increase in adsorption process of the

Table 4. Thermodynamic parameters derived for chitosan Schiff base on MS in 1 M HCl.

Concentration(ppm)	E_a kJ mol^{-1}	ΔH^*kJ mol^{-1}	ΔS^* J mol^{-1} K^{-1}
Blank	65.64	62.96	17.20
100	56.91	54.23	−18.97
300	59.47	56.80	−12.17
600	59.65	56.97	−11.81
900	59.27	56.59	−13.65
1200	59.28	56.60	−13.99
1500	60.15	57.47	−11.83

inhibitors on the metal surface and also a change in corrosion mechanism.[33,34] Enthalpy of activation ΔH^* and entropy of activation ΔS^* for the formation of activated complex are calculated by transition state equation,

$$\frac{CR}{T} = \frac{R}{Nh} \exp\left(\frac{\Delta S^*}{R}\right) \exp\left(-\frac{\Delta H^*}{RT}\right)$$

where N is the Avogadro's number, h is Planck's constant, R is molar concentration, and T is the absolute temperature. A plot of log (CR/T) against $1/T$ was constructed to obtain enthalpy and entropy of activation from slope ($-\Delta H^*/2.303RT$) and intercept, respectively. The values are listed in Table 4 and the enthalpy of activation was found to decrease in presence of the inhibitors compared to the blank solution which supports the chemisorption of inhibitor molecule.[35,36] The positive values of ΔH^* reflect the endothermic nature of dissolution of metal. The ΔH^* values are found to be less for inhibited solutions when compared to blank suggesting the slower dissolution of MS in presence of inhibitor.[37,38] The positive values of ΔS^* for the blank shows an increase in disorderliness that takes place during a metal dissolution process. Table 4 shows that the values of ΔS^* moves towards negative after the addition of inhibitor. This may be attributed to the rate determining step in which association of inhibitor molecules takes place during the activated complex formation, thus leading to a decrease in disorderliness.[39,40]

3.6. Adsorption isotherm

Basic information on the interaction between the inhibitor and the MS surface can be provided the adsorption isotherm. Surface coverage (θ) values were calculated from inhibition efficiency obtained from weight loss experiments using the relation, $\theta = IE/100$. Attempts were made to fit these θ values to various isotherm including Langmuir, Temkin, Frumkin and Freundlich. The best fit was determined using the regression values (R^2). By far, the best fit was obtained with Temkin isotherm with R^2 close to unity, Temkin adsorption isotherm is given by the equation,

$$\exp(-2a\,\theta) = KC$$

where 'a' is the molecular interaction parameter which can be negative or positive. If the values of 'a' is positive there exist the attractive force between the inhibitor molecule and if the values are negative the repulsive forces between them. θ is the surface coverage, K is the adsorption equilibrium constant, and C is the concentration of the inhibitor. When $-2a$ is represented as 'f' which describes the heterogeneity that prevail between the molecular interactions in the adsorption layer and the heterogeneity of the metal surface, Temkin equation can be represented in the transformed form as shown here,

$$\theta = \frac{1}{f} \ln K + \frac{1}{f} \ln C$$

The linear relationships of θ vs. ln C depicted in Figure 8 with regression coefficient close to unity suggest that the adsorption of the inhibitors on the metal surface followed Temkin isotherm.[41]

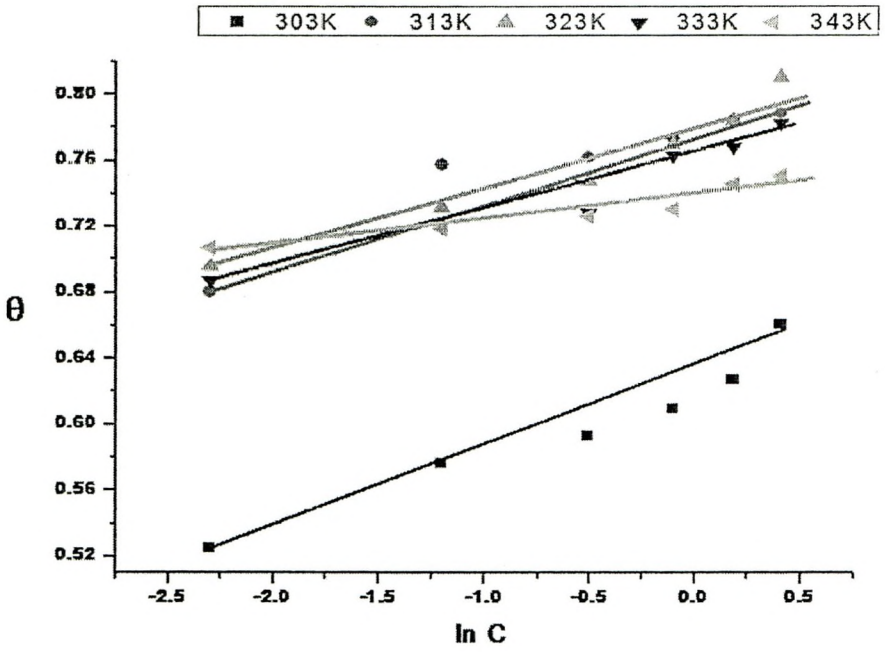

Figure 8. Temkin isotherm of chitosan Schiff base.

Temkin isotherm is basically a preliminary evidence for the chemisorptive nature of the adsorption.[29] The calculated values of *'f'* are found to be greater than zero indicating that repulsive forces exist between the adsorbed inhibitor molecules. The adsorption equilibrium constant K_{ads} signifies the strength between the adsorbent and adsorbate, larger values of K_{ads} suggests more adsorption efficiency and better inhibition performance. From the Table 5 it is observed that the K_{ads} values increase with the increase in temperature indicating the strong adsorption of inhibitor molecules onto the metal surface. Hence, the adsorptive equilibrium constant supports the chemisorption of the chitosan Schiff base on the MS surface. The thermodynamic free energy of adsorption ΔG_{ads} can be calculated using the equation, K_{ads}

$$\log K_{ads} = -log\, CH_2O - \frac{\Delta G_{ads}}{RT}$$

where CH_2O is the molar concentration of water (mol/dm^3), R is the molar gas constant (g/mol/K), and T is the temperature (K). ln K_{ads} vs. $1/T$ was plotted from which slope gives the adsorption of enthalpy ΔH_{ads} and intercept gives the adsorption of entropy ΔS_{ads} using Vant Hoff's equation,

$$\ln K_{ads} = \frac{\Delta H_{ads}}{RT} + \frac{\Delta S_{ads}}{R}$$

The values of ΔG_{ads} found to be in negative indicates that the spontaneous adsorption of the inhibitors onto the MS surface.[42] In general, if the ΔG_{ads} values are around -20 kJ mol^{-1} or lesser related to physical nature of adsorption occurring through the electrostatic interaction between the charged molecules and charged metal while the ΔG_{ads} values around -40 kJ mol^{-1} or higher related to chemical nature of adsorption that takes place due to the charge sharing or the charge transfer from the inhibitor molecules to the metal surface by forming coordinate bond.[43]

Table 5. Adsorption parameters derived for chitosan Schiff base for MS in 1 M HCl.

Temp (K)	R^2	a	f	$`K_{ads}$ dm^3 mol^{-1}
303	0.95	−0.0222	22.50	7.20×10^8
313	0.90	−0.01858	26.91	3.92×10^9
323	0.95	−0.01952	25.62	2.41×10^9
333	0.95	−0.0177	29.25	7.18×10^9
343	0.90	−0.00771	64.82	1.52×10^{13}

Temperature (K)	ΔG_{ads} (kJmol^{-1})	ΔH_{ads} (kJmol^{-1})	ΔS_{ads} (Jmol^{-1} K^{-1})
303	−45.54	585.09	2056.47
313	−62.96		
323	−60.43		
333	−66.24		
343	−130.80		

The results presented in the Table 5 indicate that ΔG_{ads} values are greater than −40 kJ mol^{-1}attributes to the strong chemical adsorption of the chitosan Schiff base on to the metal surface. It can be seen that the ΔG_{ads} values found to increase with increasing the temperature ensuring that the strong chemisorption takes place at high temperatures. The positive values of ΔH_{ads} indicate that the adsorption of chitosan Schiff base on the MS surface is endothermic. In contradiction to literature results, the positive enthalpy is associated with the positive entropy. This may be explained that the chitosan Schiff base is a long-chain polymeric compound with hetero atoms and more adsorption sites; hence before adsorbing onto the metal surface, Schiff base polymer should orient itself in the solution phase to extend the bonding with the metal surface. Thus, for the orientation of the polymer some energy is required, that exceeds the exothermic energy of the ions which adsorbs on the metal surface.[44,45] The total enthalpy of the system is an algebraic sum of adsorption enthalpy and desorption enthalpy. Thus, desorption of the water molecules becomes implicitly an endothermic process resulting in a positive enthalpy for the whole system. Adsorption of the inhibitors from the aqueous solution is regarded as quasi-substitution process between the inhibitor in the solution phase and water molecules at the metal surface. The adsorption of inhibitors on metal surface takes place by replacing the water molecules. The total entropy is calculated as algebraic sum of adsorption of inhibitor molecules and desorption of water molecules. The gain in entropy is related with the solvent entropy. Thus, the disorderliness increases from the solvent side resulting in increased entropy.

3.7. Surface analysis

Surface morphologies of the MS specimen immersed in 1 M HCl and 1500 pppm of chitosan Schiff base for 6 h are shown in Figure 9 and their respective EDX spectrum data given in Table 6. From the micrographs, it can be observed that the surface of the MS specimen immersed in 1 M HCl appears to be corroded uniformly. The corroded pits and cracks can be seen as a result of dissolution in corrosive medium. For the specimen in presence of chitosan Schiff base, the corrosion of the MS is reduced resulting in reduction surface roughness. The smoothness of the metal surface is due to the formation of protective adsorption layer by Schiff base polymer. The atomic weight percentage of elements that observed in EDX analysis is listed in Table 6. From the Table 6, the presence of nitrogen atom in chitosan Schiff base confirms the protective layer formation on the metal surface. Also, chloride

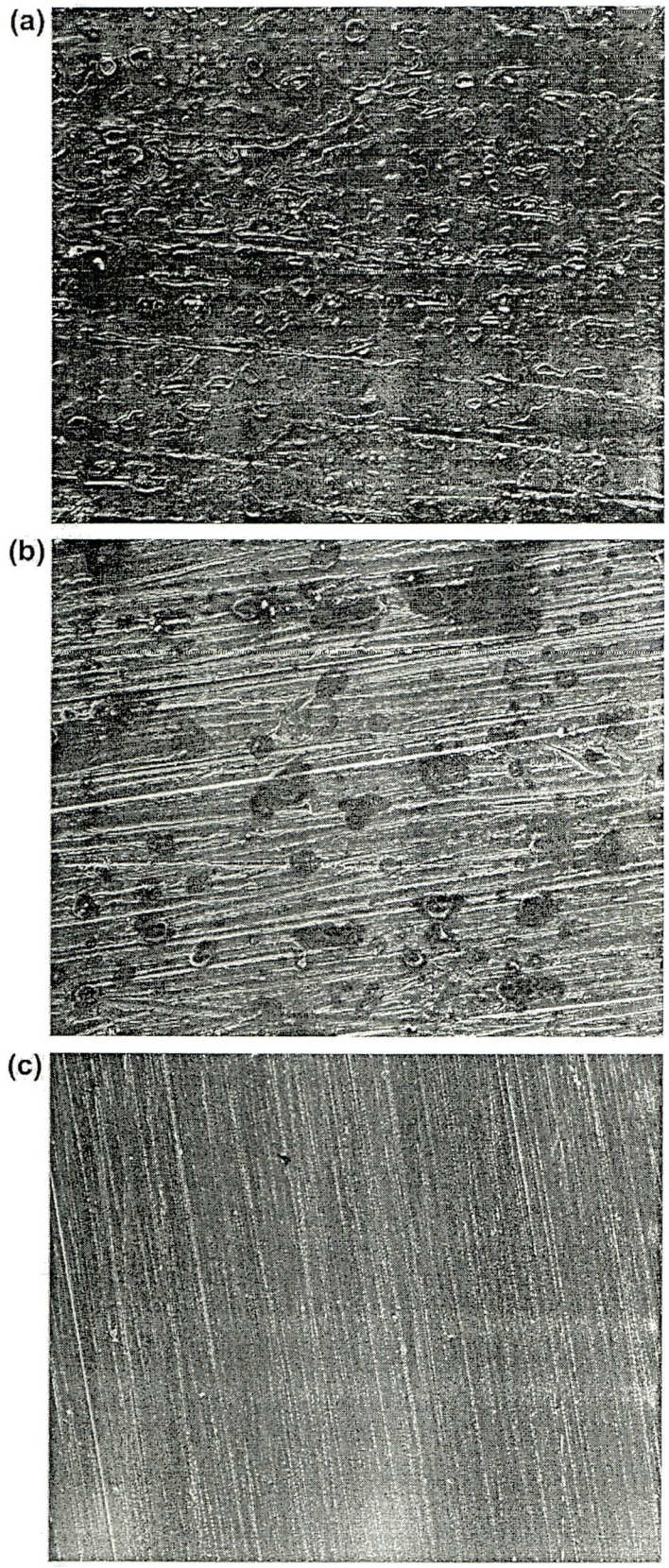

Figure 9. SEM micrographs of mild steel after 6h immersion in (a) 1 M HCl (b) 1 M HCl + CHSA (c) polished metal.

ions responsible for the metal dissolution are absent and the decrease in oxygen confirms the reduction of oxide formation on the metal surface. Moreover, it can be seen that the polymer clusters extensively cover the MS surface thus preventing the corrosion of metal in presence of inhibitor.

3.8. Mechanism of corrosion inhibition

From the experimental results, it is clear that the chitosan Schiff base reduces the MS dissolution in 1 M HCl. The thermodynamic parameters calculated revealed the chemisorption of chitosan Schiff base on the MS surface. Generally in acid medium, the anodic dissolution of iron is accompanied by the cathodic hydrogen evolution reaction as follows:

$$Fe \rightarrow Fe^{2+} + 2\,e^{-}$$

$$2H^{+} + 2e^{-} \rightarrow H_2$$

The plausible mechanism for the adsorption of inhibitor molecule on the metal surface shown in Figure 10 and can be proposed as follows: the chemical structure of the chitosan Schiff base reveals the presence of –C=N, –OH functional groups, and the chitosan repeating unit with $-NH_2$ and –OH groups. It could be assumed that the some of these groups can be protonated in acid environment and the cationic form of chitosan and chitosan Schiff base may adsorb on the cathodic sites of MS surface. On the other hand, –C=N and –OH groups have lone pair of electrons and can be adsorbed on the anodic sites of the metal surface through chemical interaction with the empty d orbitals of the metal atom. The π

Table 6. Atomic weight percentage of elements observed in EDX analysis.

	Atomic weight %				
Surface analyzed	Fe	O	Cl	C	N
Polished	78	06		15	
Blank	33	64	03	–	–
CHSA	54	30	–	12	03

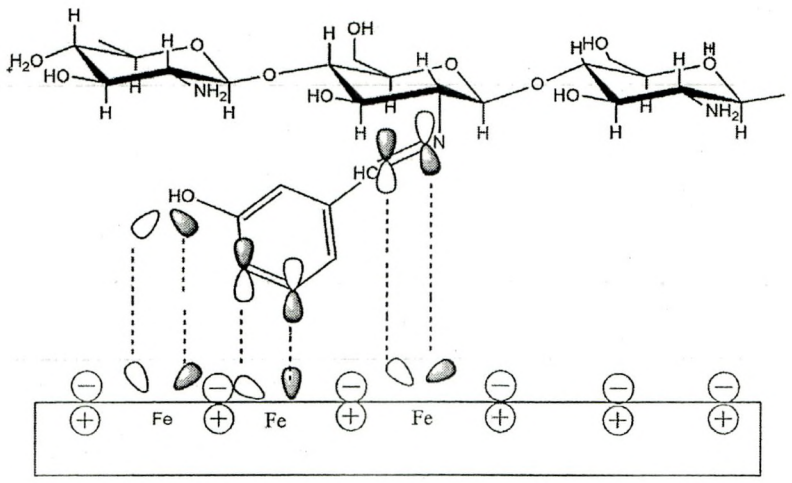

Figure 10. Schematic representation of plausible interaction of inhibitor with the metal surface.

electrons of the benzene ring (salicylaldehyde) can also interact with the MS surface by sharing electrons with the metal atom. Thus, the chitosan Schiff base inhibits the MS surface by chemical adsorption by forming coordinate bond between the active sites and vacant d-orbitals of MS surface.

4. Conclusion

Chitosan Schiff base acted as an efficient inhibitor in 1 M HCl. Polarization studies showed that the Schiff base was mixed type inhibitor. Its inhibition efficiency increased with the inhibitor concentration. The *IE* of the Schiff base was temperature depended and its addition led to decrease of the activation corrosion energy. Adsorption of the Schiff base on the MS followed Temkin adsorption isotherm indicating the inhibition process occurs via chemical adsorption. The obtained ΔG_{ads} values reveal that the corrosion inhibition by the chitosan Schiff base is mainly due to the formation of chemisorbed film on the metal surface. SEM image and EDX analysis confirmed the film formation. Two modes of adsorption can be considered: chitosan Schiff base is adsorbed on the MS surface due to the free electron pairs on the *N* atoms as well as π electrons of the aromatic rings that can interact with vacant d orbitals of iron and in the form of protonated species with already adsorbed anions.

Acknowledgement

The authors wish to acknowledge the Avinashilingam Institute for Home science and Higher Education University for Women, Coimbatore for providing lab facilities. One of the author thanks UGC for the financial support.

Disclosure statement

No potential conflict of interest was reported by the authors.

References

[1] Kalaiselvi P, Chellammal S, Palanichamy S. Artemisia pallens as corrosion inhibitor for mild steel in HCl medium. Mater. Chem. Phys. 2010;120:643–648.
[2] Khadraoui A, Khelifa A, Boutoumi H. Mentha pulegium extract as a natural product for the inhibition of corrosion. Part I: electrochemical studies. Nat. Prod. Res. 2014;28:1206–1209.
[3] Priya VS, Ali Fathima Sabirneeza A, Subhashini S. Inhibition of mild steel corrosion in sulphuric acid using Ceiba pentandra seed extract. Int. J. Curr. Res. 2014;5:6571–6575.
[4] Ashassi-Sorkhabi H, Majidi MR, Seyyedi K. Investigation of inhibition effect of some amino acids against steel corrosion in HCl solution. Appl. Surf. Sci. 2004;225:176–185.
[5] Eddy NO, Ebenso EE, Ibok UJ. Adsorption, synergistic inhibitive effect and quantum chemical, studies of ampicillin (AMP) and halides for the corrosion of mild steel in H_2SO_4. J. Appl. Electrochem. 2010;40:445–456.
[6] Eddy NO, Odoemelam SA, Ekwumemgbo P. Inhibition of the corrosion of mild steel in H_2SO_4 by penicillin G. Sci. Res. Essay. 2009;1:33–38.
[7] Geethanjali R, Ali Fathima Sabirneeza A, Subhashini S. Water-soluble and biodegradable pectin-grafted polyacrylamide and pectin-grafted polyacrylic acid:electrochemical investigation of corrosion-inhibition behaviour on mild steel in 3.5% NaCl media. Ind. J. Mat. Sci. 2014; ID 356075, p. 9.

[8] Mobin M, Khan MA, Parveen M. Inhibition of mild steel corrosion in acidic medium using starch and surfactants additives. J. Appl. Polym. Sci. 2011;121:1558–1565.
[9] Umoren SA, Obot IB, Madhankumar A, et al. Performance evaluation of pectin as ecofriendly corrosion inhibitor for X60 pipeline steel in acid medium : experimental and theoretical approaches. Carbohydr. Polym. 2015;124:280–291.
[10] Bentrah H, Rahali Y, Chala A. Gum Arabic as an eco-friendly inhibitor for API 5L X42 pipeline steel in HCl medium. Corros. Sci. 2014;82:426–431.
[11] Abdallah M. Guar gum as corrosion inhibitor for carbon steel in sulfuric acid solutions. Portugaliae Electrochim. Acta. 2004;22:161–175.
[12] Umoren SA. Inhibition of aluminium and mild steel corrosion in acidic medium using Gum Arabic. Cellulose. 2008;15:751–761.
[13] Umoren SA, Eduok UM. Application of carbohydrate polymers as corrosion inhibitors for metal substrates in different media: a review. Carbohydr. Polym. 2016;140:314–341.
[14] Umoren SA, Banera MJ, Alonso-Garcia T, et al. Inhibition of mild steel corrosion in HCl solution using chitosan. Cellulose. 2013;20:2529–2545.
[15] El-Haddad MN. Chitosan as a green inhibitor for copper corrosion in acidic medium. Int. J. Biol. Macromol. 2013;55:142–149.
[16] Waanders FB, Vorster SW, Geldenhuys AJ. Biopolymer corrosion inhibition of mild steel: electrochemical/mössbauer results. Hyperfine Interact. 2002;139/140:133–139.
[17] Cheng S, Chen S, Liu T, et al. Carboxymenthylchitosan as an ecofriendly inhibitor for mild steel in 1 M HCl. Mater. Lett. 2007;61:3276–3280.
[18] Alsabagh AM, Elsabee MZ, Moustafa YM, et al. Corrosion inhibition efficiency of some hydrophobically modified chitosan surfactants in relation to their surface active properties. Egypt. J. Pet. 2014;23:349–359.
[19] Mohamed RR, Fekry AM. Antimicrobial and anticorrosive activity of adsorbents based on Chitosan Schiff's base. Int. J. Electrochem. Sci. 2011;6:2488–2508.
[20] ASTM G 1-2. Wear and erosion; metal corrosion, Annual book of ASTM standards (vol 0.3.02). West Conshohocken: ASTM; 1996. p 89–95
[21] Wang J, Lian Z, Wang H, et al. Synthesis and antimicrobial activity of Schiff base of chitosan and acylated chitosan. J. Appl. Polym. Sci. 2012;123:3242–3247.
[22] Anan NA, Hassan SM, Saad EM, et al. Preparation, characterization and pH-metric measurements of 4-hydroxysalicylidenechitosan Schiff-base complexes of Fe(III), Co(II), Ni(II), Cu(II), Zn(II), Ru(III), Rh(III), Pd(II) and Au(III). Carbohydr. Res. 2011;346:775–793.
[23] Guinesi LS, Cavalheiro ÉTG. Influence of some reactional parameters on the substitution degree of biopolymeric Schiff bases prepared from chitosan and salicylaldehyde. Carbohydr. Polym. 2006;65:557–561.
[24] Dos Santos JE, Dockal ER, Cavalheiro ÉTG. Synthesis and characterization of Schiff bases from chitosan and salicylaldehyde derivatives. Carbohydr. Polym. 2005;60:277–282.
[25] Sashikala S, Shafi SS. Synthesis and characterization of chitosan Schiff base derivatives. Der Pharma. Lettre. 2014;6:90–97.
[26] Sasikumar Y, Adekunle AS, Olasunkanmi LO, et al. Experimental, quantum chemical and Monte Carlo simulation studies on the corrosion inhibition of some alkyl imidazolium ionic liquids containing tetrafluoroborate anion on mild steel in acidic medium. J. Mol. Liq. 2015;211:105–118.
[27] Umoren SA, Obot IB, Madhankumar A, et al. Effect of degree of hydrolysis of polyvinyl alcohol on the corrosion inhibition of steel: theoretical and experimental studies. J. Adhes. Sci. Technol. 2015;29:271–295.
[28] Lebrini M, Lagrenée M, Vezin H, et al. Experimental and theoretical study for corrosion inhibition of mild steel in normal hydrochloric acid solution by some new macrocyclic polyether compounds. Corros. Sci. 2007;49:2254–2269.
[29] Geethanjali R, Subhashini S. Thermodynamic characterization of metal dissolution and adsorption of polyvinyl alcohol-grafted poly(Acrylamide- Vinyl Sulfonate) on mild steel in hydrochloric acid. Portugaliae Electrochim. Acta. 2015; 33:35–48.

[30] Bentiss F, Traisnel M, Gengembre L, et al. A new triazole derivative as inhibitor of the acid corrosion of mild steel: electrochemical studies, weight loss determination, SEM and XPS. Appl. Surf. Sci. 1999;152:237–249.
[31] Obot IB, Madhankumar A, Umoren SA, et al. Surface protection of mild steel using benzimidazole derivatives: experimental and theoretical approach. J. Adhes. Sci. Technol. 2015;29:2130–2152. doi: 10.1080/01694243.2015.1058544
[32] Mistry BM, Jauhari S. Corrosion inhibition of mild steel in 1 N HCl solution by Mercapto-corrosion inhibition of mild steel in 1 N HCl Solution by Mercapto-quinoline Schiff base. Chem. Eng. Comm. 2014; 37–41.
[33] Khaled KF. Studies of the corrosion inhibition of copper in sodium chloride solutions using chemical and electrochemical measurements. Mater. Chem. Phys. 2011;125:427–433.
[34] Umoren SA, Obot IB, Obi-Egbedi NO. Raphia hookeri gum as a potential eco-friendly inhibitor for mild steel in sulfuric acid. J. Mater. Sci. 2009;44:274–279.
[35] Akalezi CO, Enenebaku CK, Oguzie EE. Application of aqueous extracts of coffee senna for control of mild steel corrosion in acidic environments. Int. J. Ind. Chem. 2012;3:13.
[36] Oguzie EE. Influence of halide ions on the inhibitive effect of congo red dye on the corrosion of mild steel in sulphuric acid solution. Mater. Chem. Phys. 2004;87:212–217.
[37] Sabirneeza A, Subhashini S. Poly(vinyl alcohol–proline) as corrosion inhibitor for mild steel in 1M hydrochloric acid. Int. J. Ind. Chem. 2014;5:111–120.
[38] Benabdellah M, Tounsi A, Khaled KF, et al. Thermodynamic, chemical and electrochemical investigations of 2-mercapto benzimidazole as corrosion inhibitor for mild steel in hydrochloric acid solutions. Arab. J. Chem. 2011;4:17–24.
[39] Tao Z, He W, Wang S, et al. A study of differential polarization curves and thermodynamic properties for mild steel in acidic solution with nitrophenyltriazole derivative. Corros. Sci. 2012;60:205–213.
[40] Singh P, Quraishi MA, Ebenso EE. Thiourea-formaldehyde polymer a new and effective corrosion inhibitor for mild steel in hydrochloric acid solution. Int. J. Electrochem. Sci. 2014;9:4900–4912.
[41] Umoren SA, Ebenso EE. Blends of poly vinyl pyrrolidone and polyacrylamide as corrosion inhibitors for aluminium in acidic medium. Indian. J. Chem. Technol. 2008;15:355–363.
[42] Khaled KF, El-Maghraby A. Experimental, Monte Carlo and molecular dynamics simulations to investigate corrosion inhibition of mild steel in hydrochloric acid solutions. Arab. J. Chem. 2014;7:319–326.
[43] Hosseini M, Mertens SFL, Arshadi MR. Synergism and antagonism in mild steel corrosion inhibition by sodium dodecylbenzenesulphonate and hexamethylenetetramine. Corros. Sci. 2003;45:1473–1489.
[44] Singh AK, Quraishi MA. Effect of Cefazolin on the corrosion of mild steel in HCl solution. Corros. Sci. 2010;52:152–160.
[45] Wang X, Yang H, Wang F. A cationic gemini-surfactant as effective inhibitor for mild steel in HCl solutions. Corros. Sci. 2010;52:1268–1276.